EAI Endorsed Transactions
on Pervasive Health and Technology
Research Article ICST.ORG

Cardiac and Respiratory Parameter Estimation Using Head-mounted Motion-sensitive Sensors

J. Hernandez[1,*], Y. Li[2], J. M. Rehg[2] and R. W. Picard[1]

[1] Media Lab, Massachusetts Institute of Technology, Cambridge, MA 02139 USA
[2] Center for Behavior Imaging and the School of Interactive Computing, Georgia Institute of Technology, Atlanta, GA 30332 USA

Abstract

This work explores the feasibility of using motion-sensitive sensors embedded in Google Glass, a head-mounted wearable device, to robustly measure physiological signals of the wearer. In particular, we develop new methods to use Glass's accelerometer, gyroscope, and camera to extract pulse and respiratory waves of 12 participants during a controlled experiment. We show it is possible to achieve a mean absolute error of 0.82 beats per minute (STD: 1.98) for heart rate and 0.6 breaths per minute (STD: 1.19) for respiration rate when considering different observation windows and combinations of sensors. Moreover, we show that a head-mounted gyroscope sensor shows improved performance versus more commonly explored sensors such as accelerometers and demonstrate that a head-mounted camera is a novel and promising method to capture the physiological responses of the wearer. These findings included testing across sitting, supine, and standing postures before and after physical exercise.

Keywords: Ballistocardiography (BCG), blood volume pulse (BVP), heart rate, respiration rate, head-mounted wearable device, gyroscope, accelerometer, camera, daily life monitoring.

Received on 31 October 2014, accepted on 20 February 2015, published on 18 May 2015

doi: 10.4108/phat.1.1.e2

1. Introduction

Being able to comfortably monitor physiological information during daily life can reduce the costs associated with health measurement and care delivery [37]. For instance, physiological measures such as cardiovascular and respiratory activity can be used for early detection and diagnosis of relevant risk factors of cardiovascular disease [6] as well as for helping to monitor chronic conditions and therapeutic interventions.

Traditional approaches to measure parameters such as heart rate require attaching electrodes to the skin, which is cumbersome for daily life monitoring. However, recent advances in technologies have enabled the creation of wearable devices of reduced sized, weight and power consumption. These devices are in close contact with the body and offer a new set of low-cost unobtrusive sensors that can run continuously during daily activities.

In this work we focus on the motion-sensitive capabilities within a commercial product, the Google Glass (see Fig. 1). Google Glass is a wireless head-mounted device equipped with a touch pad, a see-through display, and most of the sensors available in smartphones. Although the device was not designed for physiological measurement, its unique location on the head of the person provides an opportunity to unobtrusively monitor physiological information during daily activities. In particular, we develop new methods allowing the gyroscope, the accelerometer and the camera embedded in Glass to be used to capture subtle head motions of the wearer that are associated with the mechanical activity of the heart and the respiration of the wearer.

*Corresponding author. Email:javierhr@mit.edu

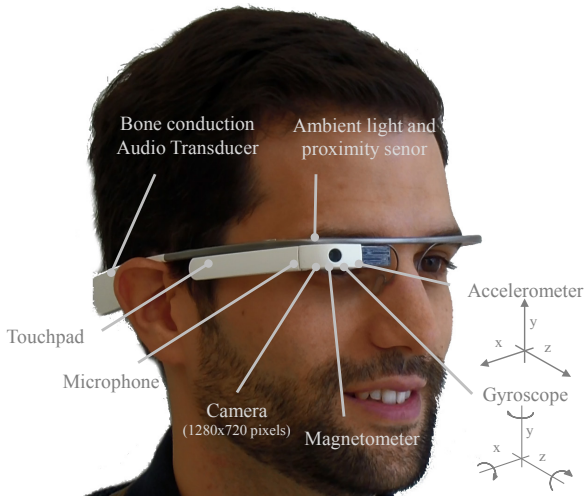

Figure 1. Head-mounted wearable device Google Glass and the locations of some of the main sensors.

The paper is organized as follows. We start by reviewing the previous literature on non-invasive physiological measurement, followed by a description of the experimental setting and the sensors used in our study. Next, we present the algorithms to retrieve pulse and respiratory waves from different sensors. The results of the proposed algorithms are then compared to an FDA cleared heart rate and respiration rate sensor. Finally, we discuss the potential implications of this work for real-life monitoring.

2. Non-Invasive Physiological Measurement

One of the least invasive physiological measurement approaches is photoplethysmography (PPG) which captures color variations of reflected light on the skin. Traditional measurements of PPG require a dedicated light source in close contact with the surface of the skin such as the finger [1]. However, Verkruysse et al. [38] demonstrated that it's also possible to gather this type of information using a remote camera (>1m) and ambient light. This idea was further explored by Poh et al. [30][31] who proposed and validated a method to robustly extract physiological parameters using a regular webcam. More recently, Wu et al. [39] proposed a method to amplify and visualize frequency changes in a video. Among many explored applications, the authors used their method to amplify and visualize blood flow changes in a baby's face, along with its respiration movements. Although these studies represent some of the least invasive approaches currently available, they require having a camera pointed at the person which severely limits their possibilities for daily life monitoring. This work includes PPG measurements from the finger to provide ground truth physiological comparison.

An alternative approach that has the potential to enable non-intrusive physiological measurements is ballistocardiography (BCG). This method was popularized by Starr et al. [36] who showed that the mechanical ballistic forces of the heart elicit subtle body movements. While the original experiments required a subject to lie down on a suspended supporting structure, continuous technological advances have enabled BCG measurement in less constrained settings [9]. For instance, researchers have successfully gathered BCG information from daily life objects such as modified weighing scale [18], a chair [32] or a back pad [28]. Moreover, a wide variety of methods have been explored to gather similar information during sleep, when the amount of motion artifacts are minimized (e.g., [4][5][24][27][34]). Researchers have also started to consider more wearable approaches which are more appropriate for daily life monitoring. For instance, Kown et al. [20] and Dinh [7] attached a smartphone to the chest and used its accelerometer to monitor heart rate. Similarly, Phan et al. [29] proposed a different approach to extract heart rate and respiration. While these approaches enable measurements during daily life, they mostly focus on the chest location where both cardiac and respiratory motions are more prominent. In a series of studies, however, He et al. [11][12][13] created a custom-made device and demonstrated that heart rate could also be extracted from a peripheral location such as the ear. In [14], He also showed preliminary results of respiration rate estimation from accelerometer data for a single sample but no validation was performed. This work similarly demonstrates that heart rate can be performed from accelerometer data but also provides a methodological validation of respiration rate estimation. Moreover, we show improvements with novel use of the gyroscope, and explore a different peripheral location of the sensor (above the right eye instead of over the ear). Finally, our work also considers the use of a head-worn camera that captures the egocentric view of the person to monitor subtle periodic motions. This is in contrast to the work of Balakrishnan et al. [2], which measured the heart rate of a person in front of a static camera by monitoring subtle head motions. To the best of our knowledge, the work presented here is the first to use the egocentric view of a wearer to gather his or her own physiological data.

3. Experimental Procedure

Twelve participants (6 females) with an average age of 27.3 (STD of 5.3) years old, weight of 144.5 (STD: 30.9) pounds and height of 5.65 (STD: 0.4) feet participated in this study. After obtaining written consent, participants were asked to keep still, breathe spontaneously and look at a static indoor scene situated at a distance of 2.2 meters while remaining in three different positions (standing up, sitting down and lying down) for a minute each. In order to generate a larger dynamic range of physiological readings, participants were then asked to repeat the three positions after pedaling a

stationary bike for one minute. Thus, this procedure provided 72 minutes of well-characterized data over a range of heart rate and respiratory conditions. At the end of the study, participants took a survey and were compensated with a $5 Amazon gift card.

We created a custom Android application to simultaneously log information from the accelerometer, the gyroscope and the camera of an early beta version of Google Glass. In order to measure the ground truth physiology, participants also wore an FDA cleared sensor (FlexComp Infiniti by Thought Technologies) that simultaneously recorded Blood Volume Pulse (BVP) from the finger and respiration from a chest belt sensor at a constant sampling rate of 256 Hz. The Institutional Review Board of the Massachusetts Institute of Technology approved the study.

4. Sensors and Preprocessing

This work explores the utility of three different sensors embedded in a head-mounted device. In the following, we provide a brief description of each sensor and some of the main considerations.

4.1. Accelerometer

The 3-axis accelerometer captures the acceleration applied to the device (meters/second^2) along the X, Y and Z axes (see Fig. 1). Accelerometer measurements include the force of gravity and have been widely used in the context of activity recognition [21]. Furthermore, this sensor seems to be one of the preferred choices to sense BCG measurements in different contexts [7][11][20][29][33]. In our specific setting, we were able to retrieve accelerometer information at an average sampling rate of 50 Hz. In order to ensure a constant sampling rate, we performed cubic interpolation at a sampling rate of 256 Hz (the same as the FlexComp Infiniti sensor). There were some sporadic cases where the sensor did not log any data for long periods of time (e.g., half a second), which introduced critical artifacts when estimating physiological information. We believe part of the problem was due to the simultaneous logging of the three sensors and the limited capability of the beta version of Google Glass to handle high sampling rates. To minimize the effect of these artifacts, we applied a hard-thresholding method (2 STD above and below the mean) for each observation window.

4.2. Gyroscope

The 3-axis gyroscope captures the rate of rotation (radians/second) of the device along the X, Y and Z axis of the device (see Fig. 1). Unlike an accelerometer, a gyroscope is not affected by gravity but may present a cumulative error (drifting) when analyzed over time. A common application of this sensor is the stabilization of aerial vehicles, but it can also be combined with other sensors to provide accurate localization (e.g., [19]). To the best of our knowledge this sensor has not been validated in the context of BCG measurement, probably due to the limited rotational motions of considered body locations (e.g., chest, ear). Similarly to the accelerometer sensor, the average sampling rate of the gyroscope was 50 Hz and sensor drops were sometimes observed. We applied the same cubic interpolation and thresholding described above.

4.3. Camera

The video was recorded at a constant frame rate of 30Hz at a resolution of 1280x720 pixels (the default settings of Glass). Each of the pixels yields a vector in RGB color space. We estimate the motion of the device by tracking 2D feature points in the video. First, we detect feature points [34] in each frame and track them using a Kanade-Lucas-Tomasi feature tracker [22]. We then fit a homography matrix [10] to the point correspondences using RANSAC [8]. We assume that all tracked points correspond to static 3D points, in which case their offsets are solely explained by the camera motion. Finally, the vertical and horizontal motion (up to a scale) of the camera can then be directly extracted from the matrix. While more accurate motion estimation methods exist (e.g., [10]), they require addressing additional challenges such as calibrating the camera and facing degenerate conditions for small movements that may attenuate the physiological information. To the best of our knowledge, this work is the first to use the egocentric view of a wearer to gather his or her own physiological data.

5. Physiological Parameter Estimation

A challenge in extracting physiological parameters during daily activity with wearable devices is to develop algorithms that require low-computational power and run in real-time. Therefore, we constrained our new methods to use combinations of efficient signal processing techniques. In this section we provide details about the proposed processing steps to estimate the pulse and respiratory waves from a specific stream of sensor data.

5.1. Pulse Wave

Given a specific sensor modality with sensor readings as a time series of vectors (e.g., 3D vector for accelerometer and gyroscope, 2D vector for camera), the estimation of the pulse wave was divided into the following steps:

(i) A moving average window of 3 samples was subtracted from each dimension of the

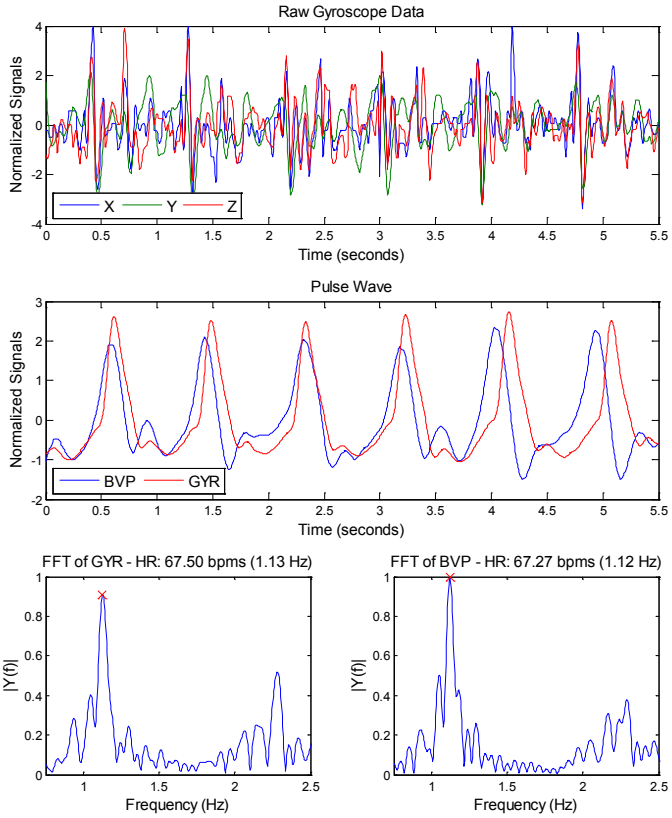

Figure 2. Example of an estimated pulse wave from gyroscope data (red) and the ground truth blood volume pulse signal (blue). Bottom graphs show the Fourier Spectrum of each signal. (FFT: Fourier Spectrum, GYR: Gyroscope, BVP: Blood Volume Pulse, HR: Heart Rate, bpms: beats per minute)

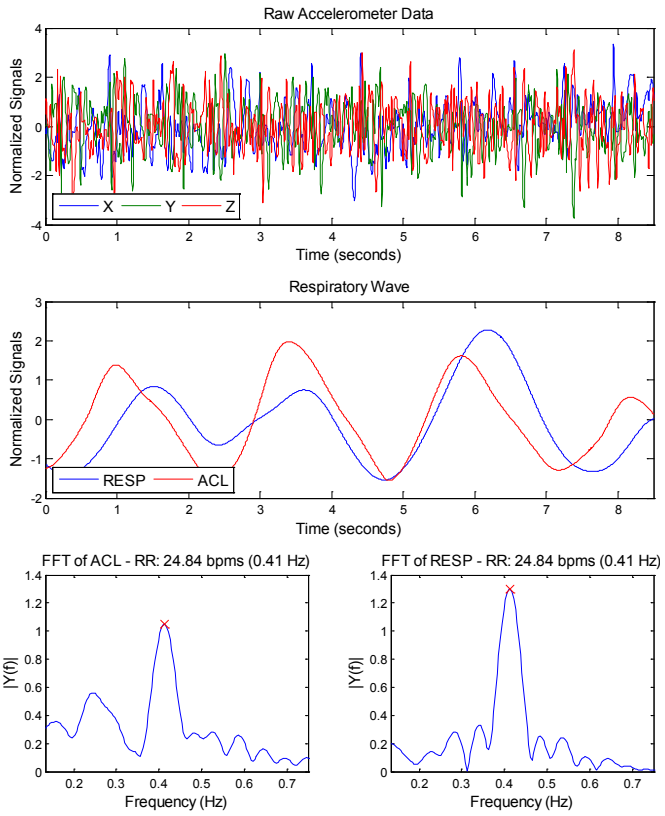

Figure 3. Example of an estimated respiratory wave from accelerometer data (blue) and the ground truth respiration signal (red). Bottom graphs show the Fourier Spectrum of each signal. (FFT: Fourier Spectrum, ACL: accelerometer, RESP: Respiration from chest band, RR: respiration rate, bpms: breaths per minute)

vector, allowing the removal of signal shifts and trends.

(ii) A band-pass Butterworth filter of order 4 with cut-off frequencies of 10 and 13 Hz was applied to each dimension to isolate BCG changes.

(iii) In order to aggregate the different components of the signal, i.e. dimensions of the vector, we compute the square root of the summation of the squared components (i.e., L2 norm) at each sample. This aggregation gives the same relevance to each of the dimensions and makes our approach more robust to different body postures.

(iv) Finally, a band-pass Butterworth filter of order 2 with cut-off frequencies of 0.75 and 2.5 Hz (corresponding to 45 and 150 beats per minute) was applied, yielding the final pulse wave.

Fig. 2 shows an example of pulse wave estimation from gyroscope data of a person wearing the head-mounted wearable device while lying down. The top graph shows the 3-axis gyroscope over a period of 5.5 seconds and clearly shows the BCG changes. The middle graph shows the pulse wave obtained by BVP (blue) and the pulse wave obtained after applying the described methods on the gyroscope data (red line). As can be seen, the estimated pulse wave is well aligned with the wave of reference and is able to capture the changes associated with the beats and their reflections.

5.2. Respiratory Wave

In order to estimate the respiratory wave from data of a specific sensor (same to what we used for pulse wave), we performed the following steps independently for each sensor modality:

(i) An averaging filter was applied to each of the components. The window length was set to be the duration of a respiration cycle at a maximum breathing rate (45 breaths per minute in our case).

(ii) A band-pass Butterworth filter of order 4 with cut-off frequencies of 0.13 and 0.75 Hz (corresponding to 8 and 45 breaths per minute) was applied to each dimension.

(iii) Since different dimensions of the sensor reading (e.g., X and Y axis of accelerometer) may change in different directions depending on the body position, we applied Principal Component Analysis to reduce this influence. We then computed the Fast Fourier

Transform of each principal component and selected the most periodic signal, where periodicity of the signal was estimated by computing the maximum magnitude observed within the operational frequency range.

Fig. 3 shows an example of respiratory wave frequency estimation from accelerometer data of a supine participant. As in Fig. 2, the two waves are closely aligned.

5.3. Heart and Respiration Rates

For each of the waves we extracted the heart rate and the respiration rate in the frequency domain. Given an estimated wave or ground truth signal, we extracted the frequency response with the Fast Fourier Transform and identified the frequency with the highest amplitude response. The band of frequencies used for the pulse and respiration rates are the same ones considered in the previous section (i.e., [0.75-2.5] Hz for heart rate and [0.13-0.75] Hz for respiration rate). The final estimated heart rate and respiration rate corresponded to the maximum frequency multiplied by 60 (beats per minute). Computing these parameters in the frequency domain instead of the time domain allowed us to 1) partially address the problem of missing peaks due to non-constant sampling rates of accelerometer and gyroscope, 2) deal with the non-linear phase responses of the Butterworth filter, and 3) avoid addressing the problem of peak detection. Future work will focus on ensuring more constant sampling rates and the development of more computationally efficient and robust-to-extraneous-movement peak detection.

The bottom graphs of Figs. 2 and 3 show the Fourier Spectrum over the whole 20 second estimated (left) and reference (right) waves. As can been seen, the frequency responses for the two waves are closely aligned and their maximum frequency response is approximately the same: 1.1 Hz (corresponding to a heart rate of 62 beats per minute) for the pulse waves, and 0.41 Hz (corresponding to 25 breaths per minute) for the respiratory waves.

6. Results

Each of the 12 participants held three different positions under relaxed and aroused (after biking) conditions for a minute each. Therefore, we collected 72 1-minute segments of data. In order to increase the number of samples, we divided the data into intervals of 20 seconds with a 75% overlap, yielding 648 samples. In this section, we use the segmented data to compare performance across the three modalities and body postures. We then evaluate the benefit of combining the three modalities. Finally, we explore the effects of dividing the data into intervals of different durations.

6.1. Comparison across Modalities

To evaluate the utility of each sensor modality, we extracted heart rate and respiration rate from each of the samples and computed the same performance metrics used in Poh et al. [31]. Fig. 4 shows the Bland-Altman plots [3] for each physiological parameter using the different modalities. In particular, each graph shows the agreement of the 648 pairs of measurements color-coded by participant. The graphs also show the mean error and the 95% limits of agreement (i.e., 1.96 standard deviations above and below the mean). As can be observed, most of the graphs have a significant concentration of points along the zero values of y-axis, illustrating a close agreement between the measurements. Tables 1 and 2 show a summary of quantitative metrics for heart rate and respiration rate, respectively, across all the 648 segments (72 minutes) of data computed from the 12 participants. We observe the same trend across three modalities for both heart rate and respiration rate: our estimation has a high accuracy in comparison to ground-truth, while the errors vary across different sensors. The small mean errors from different modalities provide strong evidence to the feasibility of our approach. When comparing the three sensors individually, the gyroscope yielded the best performance for both heart and respiration rates, achieving a mean absolute error of 0.82 beats per minute (STD: 1.98) and 1.39 breaths per minute (STD: 2.27), respectively. Notably, the accelerometer (upon which prior BCG work is based) was never the best performing modality for heart rate or respiration. While the camera modality outperformed the accelerometer for estimating respiration rate (achieving a ME of 1.55 breaths per minute), its performance for heart rate estimation was the worst (ME: 7.92 beats per minute).

The process of extracting motion measurement from video is more complex and less direct than it is for the other two sensors. For instance, different factors such as the depth of the scene or the amount of feature points that can be tracked in the environment have a direct impact on the performance. Furthermore, the sampling rate of the camera was significantly lower than the other two sensors. Therefore, high frequency changes such as subtle head movements due to heart activity may not be as accurately captured as the low frequency movements associated with respiration. While these results still show that it's possible to extract heart and respiratory information from the egocentric video of the wearer, future work will focus on performing a more systematic comparison across different factors, e.g. motion estimation method, depth of the scene and objects, amount of tracked points.

6.2. Postural Changes

Body posture mediates the intensity and quality of BCG movements. In this study, participants were measured from

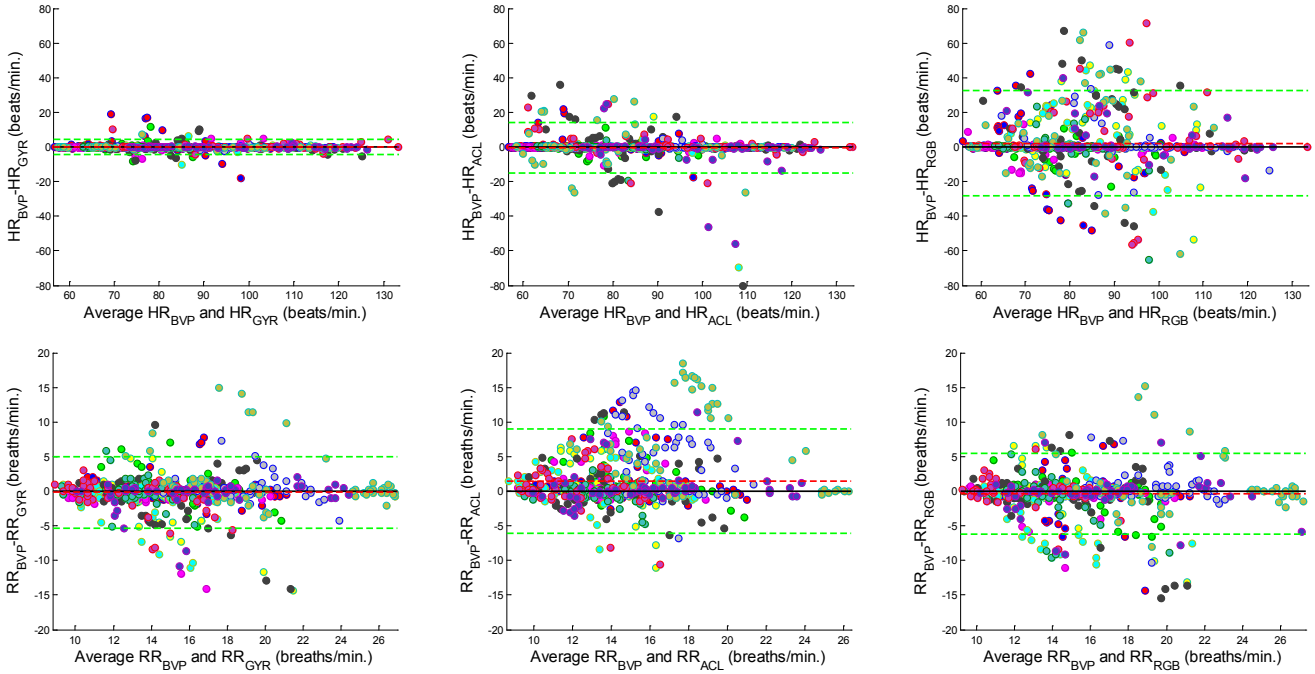

Figure 4. Bland-Altman plots for heart (top) and respiration rates (bottom) using gyroscope (left), accelerometer (center), and camera (right). Each graph shows the agreement of 648 pairs of measurements. Data from different participants are represented with dots of different colors. Mean error is depicted with slashed red and 95% limits are depicted with slashed green lines. (HR: Heart Rate, RR: Respiration Rate, GYR: Gyroscope, ACL: Accelerometer, RGB: Camera)

Table 1. Heart Rate Estimation

Sensor	ME	STD	RMSE	CC
Gyroscope	0.82	1.98	2.14	0.99
Accelerometer	2.51	7.03	7.46	0.91
Camera	7.92	13.4	15.56	0.58
All	1.19	3.42	3.62	0.98

Table 2. Respiration Rate Estimation

Sensor	ME	STD	RMSE	CC
Gyroscope	1.39	2.27	2.66	0.75
Accelerometer	2.29	3.43	4.12	0.41
Camera	1.55	2.59	3.02	0.69
All	1.16	2.04	2.35	0.79

ME = Mean absolute error (beats/breaths per minute)
STD = Standard deviation of the absolute error
RMSE = Root mean squared error
CC = Pearson's correlation coefficient

three body postures: sitting, standing, and supine. Tables 3 and 4 show the mean absolute error (beats and breaths per minute, respectively) for each of the different positions and sensors. When estimating heart rate, the most challenging position was sitting down, which is in accordance with the results described in [11]. The results obtained with the gyroscope in this study outperform the results of He et

Table 3. Mean Absolute Error of Heart Rate

Sensor	Sitting	Standing	Supine
Gyroscope	1.18	0.85	0.44
Accelerometer	3.30	2.18	2.06
Camera	4.51	10.17	9.10
All	1.48	1.17	0.92

Table 4. Mean Absolute Error of Respiration Rate

Sensor	Sitting	Standing	Supine
Gyroscope	1.13	1.97	1.06
Accelerometer	1.87	3.17	1.82
Camera	1.32	1.89	1.45
All	0.94	1.77	0.77

al. [11] for the sitting (ME: 1.27) and supine (ME: 0.84) conditions but not for the standing (ME: 0.72) position. However, the range of heart rates they observed in their study was considerably smaller (55 to 95 beats per minute) in comparison to the ones we elicited (56 to 133 beats per minute). The different results for the camera sensor may be due to a combination of several factors such as the influence of body posture, the accuracy of motion estimation as well as the relative pose of the camera with

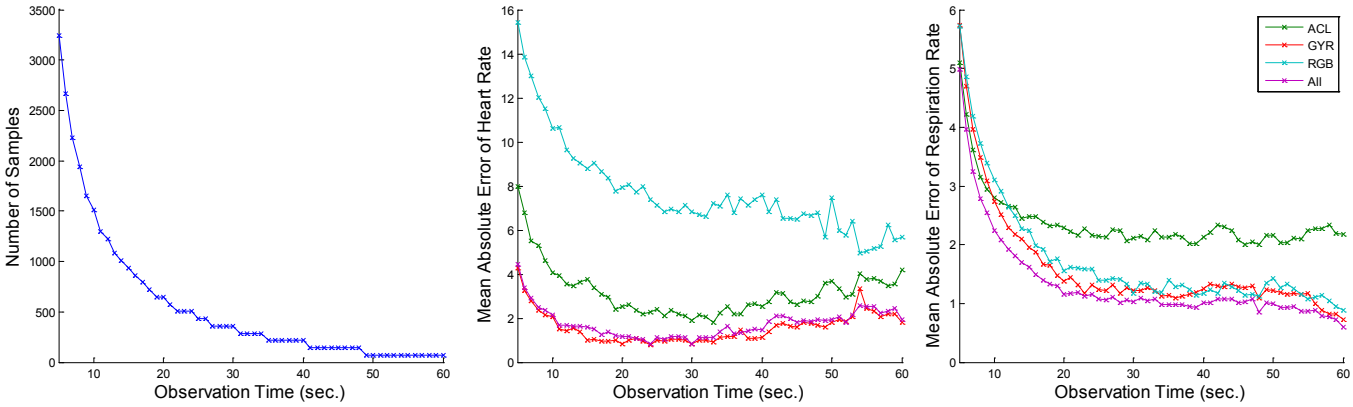

Figure 5. Mean absolute error for heart (beats per minute) and respiration rates (breaths per minute) when considering different window sizes. (ACL: Accelerometer, GYR: Gyroscope, RGB: Camera)

respect to the wearer's head. When estimating respiration rate, the most challenging position was standing up for all the modalities. Apparently, respiratory movements have less influence on head motion while standing. Overall, even the most challenging posture positions yielded low error for the best-performing modality.

6.3. Combination of Modalities

Differences in performance across modalities are partly due to the different types of information being captured by each of the sensors. For instance, while the accelerometer data captures linear accelerations, the gyroscope captures rotations of the device. Furthermore, while some of the sensors may be affected by sampling rate artifacts (e.g., accelerometer and gyroscope), other sensors may provide more constant sampling rates but less accurate information (e.g., camera). Therefore, a combination of different modalities may help to provide more reliable estimates at the cost of computational complexity. To explore this idea, we extracted the heart/respiration rates of each modality separately and computed the median as the final estimate. The bottom rows of Tables 1 and 2 show the results using this late fusion technique. While the heart rate estimation using the gyroscope was still better than the one obtained combining all the modalities, the respiration rate estimation with all three modalities yielded better results than with any of the other modalities alone (reducing the ME to 1.16 breaths per minute, STD 2.04). Although not explored in this work, we expect larger improvements by combining physiological signals in less controlled settings where different modalities might provide complementary information about motion.

6.4. Observation Windows

While combining several sensors may partially address the problem of motion artifacts, an underlying assumption of the proposed methods and evaluation is that the person is holding a motion-less position for the majority of a certain observation window (20 seconds for the previous results). However, being able to remain still for large periods of times during daily life may not be always possible and shorter and more available observation windows may be preferred. In order to explore the performance of our methods for different lengths of observation windows, we split the collected data into segments of different durations following the same criteria described above and assessed their performance. Fig. 5 shows the number of samples obtained for each of the observation windows (left), and the absolute mean error of the different approaches to estimate heart rate (center) and respiration rate (right). As can be seen, heart rate can be computed with a ME of 4 beats per minute with an observation window of only 5 seconds from gyroscope. This error goes below 2 beats per minute for observation windows equal or larger than 10 seconds, reaching its minimum at 25 seconds. The decrease of performance with smaller windows is expected due to several factors. When computing heart and respiration rates, especially in the frequency domain, longer observation windows are preferred to provide more accurate estimates. Moreover, different body locations reflect physiological changes at different times which can negatively bias our estimates.

Although we expected ME would always decrease with longer observation windows, there was a subtle rebound effect for windows above 30 seconds for the accelerometer and gyroscope data. Visual inspection suggested that this rebound was due to missing beats due to the non-uniform sampling rates of these two sensors, which became more significant when reducing the amount of samples. This effect was not observed when estimating respiration rate, where larger observation windows always improved performance. This finding is in accordance with the previous observation as breathing rate operates in a lower frequency range and the non-uniform sampling rate did not negatively affect the signal. Using the longest observation window (60 seconds) and a combination of all the sensors, the ME was reduced to 0.6 breaths per minute (STD: 1.19).

Note that the fusion of the three modalities performs more or less the same as the best modality when estimating the heart rate, and consistently leads to slightly better results than the individual modalities when estimating respiration rate. These results are promising for real-life monitoring where the head of the person is more likely to remain still for shorter periods of time than longer ones. In practice, the duration of the observation window and the accuracy is a trade-off that needs to be carefully chosen when deciding on a specific population and/or application. For instance, children may have more problems to remain still than adults and shorter and less accurate windows may be preferred. However, longer and more accurate readings may be more accessible and adequate in certain scenarios such as sleeping or practicing meditation.

7. Discussion

The previous sections have shown that it is possible to capture physiological parameters from acceleration, gyroscope and camera. The results from different modalities are consistent and the mean absolute errors are small, which further justify our methods. Furthermore, some of our results were improved by combining several modalities and changing the observation windows. While we expect the combination of sensors will yield improved assessments of physiological parameters during daily life, there are critical differences among sensors that need to be considered.

Both accelerometer and gyroscope require considerably less energy than the camera and, therefore, allow for longer periods of monitoring without charging the batteries. With the current version of device, we were able to continuously record gyroscope and accelerometer data for around 8 hours with an average sampling rate of 50 Hz. These two sensors directly capture complementary aspects of the wearer's head motion. For instance, while driving a car, the accelerometer readings may be influenced by external forces such as changes of speed; however, the gyroscope will provide cleaner signals associated with the rotation of the head of the driver. In this specific case, the accelerometer and the gyroscope can provide meaningful information about both the context and the physiology.

The camera requires significantly more energy (the current battery lasts approximately 20 minutes of continuous monitoring), but also provides some critical benefits. The location of the camera of the head-mounted device in this work is located above the right eye (see Fig. 1). This setup offers the opportunity of capturing the environment from the wearer's perspective. This information is useful not only to extract physiological parameters as demonstrated in this work, but also to capture rich contextual information that helps infer the sources of physiological responses. For instance, a person exercising at the gym and a person giving a public presentation may show similar increases in heart and respiration rates. However, the same arousal of physiological signals is due to different reasons (physical stress vs. affective-cognitive stress). The visual context in these cases, therefore, plays a critical role to interpret the physiological signals. Furthermore, linking physiological information with visual imagery can be useful in a wide variety of applications such as catalyzing introspection [15], augmenting human memory [17], and improving social communication [23].

One of the main challenges when estimating physiological parameters from motion in real-life scenarios is the presence of large ego-motion due to physical activity. Daily activities such as walking or speaking with other people involve large body movements that might occlude the subtle heart and respiratory motions. Although this study did not directly address this issue, we evaluate our methods for a large range of observation windows. For instance, with only a 5-second observation we were able to provide estimates of heart rate with a ME of 4 beats per minute with gyroscope. This observation window is significantly smaller than windows reported on similar studies (e.g., >70 sec. in [2], >20 sec. in [11], 30 sec. in [30]). An important area of research is to understand how often these observation windows are accessible during daily life activity. In a relevant study, Rienzo et al. [33] monitored sternal seismocardiogram of 5 participants during 24 hours and found that there were more than 100 5-second segments per hour with good quality acceleration data during the day and three times higher during the night. These numbers were quickly reduced with longer observation windows. These results are promising for non-intrusive physiological assessments. However, the location and types of sensors of this study are different, and can have an impact on the statistics. Future research will assess the availability of good quality data from participants wearing a head-mounted device during daily life activity.

8. Conclusions

In this work we have explored the possibility of using different motion-sensitive sensors of a head-mounted wearable device to extract physiological parameters of the wearer. In particular, this work has 1) proposed real-time algorithms to process head-mounted motion-sensitive sensors, 2) provided validation of heart and respiration rate estimation with FDA-cleared sensors in a controlled laboratory setting, and 3) quantitatively compared sensor modalities, body postures, and observation windows.

Among the three motion-sensitive sensors we considered, we have shown that the gyroscope outperformed the other sensors, including the accelerometer upon which prior BCG measurements are mostly based (e.g., [7][11][20][29][33]). We believe this improvement is partly due to the above-eye location of the sensor and its capability to capture amplified rotational movements of BCG. Moreover, we have demonstrated that

analyzing the ego-centric view of head-mounted camera is a novel and promising method to harvest physiological information of the wearer, with the benefit of also providing insightful visual context. Finally, as each of the modalities captures different aspects of motion, their combination offers the opportunity to improve overall performance. For instance, this work has demonstrated preliminary improvements in the estimation of respiration rates when combining the estimations of the three modalities.

Future efforts will consider evaluating other modalities and developing novel methods to combine them depending on contextual information such as body postures or activities. We have also started to work on more sophisticated methods that can handle large motions associated with daily activities, which is fundamental to apply the proposed methods in real world settings. In the future, we will also be analyzing other relevant physiological parameters such as heart rate variability (e.g., [4]) as it has been shown to be associated with cognitive load [26] and stress [16][25]. The key to this parameter is to obtain highly accurate timing of the heartbeats and, therefore, uniform sampling rates and filters without phase delays will be explored.

In summary, this work has shown a new capability to provide accurate real-time heart-rate and respiration measures from motion-sensitive sensors available in today's head-mounted wearable Google Glass. With the continuous technological improvements and commercial reach of new devices, we expect our results will help facilitate non-intrusive access of meaningful physiological information during daily activity. We are looking towards a future where this type of information is more accessible and is used to enhance the delivery of primary health care and the monitoring of chronic conditions.

Acknowledgements.

This material is based upon work supported by Google, the National Science Foundation (NSF 1029585 and NSF 1029679), the MIT Media Lab Consortium, and the Intel Science and Technology Center for Pervasive Computing.

References

[1] ALLEN, J. (2007) Photoplethysmography and its application in clinical physiological measurement. *Physiological Measurement* vol. 28(3): pp. R1-R39.

[2] BALAKRISHNAN, G., DURAND, F. and GUTTAG J. (2013) Detecting Pulse from Head Motions in Video. In *Proceedings of IEEE Conference on Computer Vision and Pattern Recognition*, pp. 3430-3437.

[3] BLAND, J. M. and ALTMAN, D. G. (1986) Statistical methods for assessing agreement between two methods of clinical measurement. *Lancet,* vol. 1(8476): pp. 307–310.

[4] BRÜSER C., WINTER S., and LEONHARDT S. (2013) Robust inter-beat interval estimation in cardiac vibration signals. *Physiological Measurement*, 34 (2), pp. 123-138.

[5] BRINK M., MÜLLER C. H., and SCHIERZ C. (2006) Contact-free measurement of heart rate, respiration rate, and body movements during sleep, *Behavior Research Methods*, vol. 38 (3): pp. 511-521.

[6] COOK, S., TOGNI, M., SCHAUB, M. C., WENAWESER, P. and HESS, O. M. (2006) High heart rate: a cardiovascular risk factor? *European Heart* vol. 27 (20): pp. 2387–2393.

[7] DINH, A. (2011) Heart Activity Monitoring on Smartphone. In *Proceedings of International Conference on Biomedical Engineering and Technology*, vol. 11, pp. 45-49.

[8] FISCHLER, M. A. and BOLLES, R. C. (1981) Random sample consensus: a paradigm for model fitting with applications to image analysis and automated cartography. *Communications of the ACM*, vol. 24(6): pp. 381-395.

[9] GIOVANGRANDI L., INAN O., WIARD R., ETEMADI M, and KOVACS G. (2011) Ballistocardiography - a method worth revisiting. In *Proceedings of Engineering in Medicine and Biology Society,* pp. 4279-4282.

[10] HARTLEY, R. and ZISSERMAN, A (2004) *Multiple view geometry in computer vision.* 2nd ed. (Cambridge University Press).

[11] HE, D. D., WINOKUR, E. S. and SODINI, C. G. (2012) An ear-worn continuous ballistocardiogram (BCG) sensor for cardiovascular monitoring. In *Proceedings of Engineering in Medicine and Biology Society*, pp. 5030-5033.

[12] HE, D. D., WINOKUR, E. S. and SODINI, C. G. (2011) A Continuous, Wearable, and Wireless Heart Monitor using Head Ballistocardiogram (BCG) and Head Electrocardiogram (ECG). In *Proceedings of Engineering in Medicine and Biology Society,* pp. 4729-4732.

[13] HE, D. D., WINOKUR, E. S., HELDT, T. and SODINI, C. G. (2010) The Ear as a Location for Wearable Vital Signs Monitoring. In *Proceedings of Engineering in Medicine and Biology Society,* pp. 6389-6392.

[14] HE, D. D. (2013) A wearable heart monitor at the ear using ballistocardiogram (BCG) and electrocardiogram (ECG) with a nanowatt ECG heartbeat detection circuit. *Ph.D. dissertation*, Department of Electrical Engineering and Computer Science, Massachusetts Institute of Technology, Cambridge, MA.

[15] HERNANDEZ, J., MCDUFF, D., FLETCHER, R., and PICARD, R. W. (2013) Inside-Out: Reflecting on your Inner State. In *Proceedings of Pervasive Computing and Communications Workshops*, pp. 324-327.

[16] HJORTSKOV, N., RISSEN, D., BLANGSTED, A. K., FALLENTIN, N. LUNDBERG, U. and SØGAARD, K. (2004) The effect of mental stress on heart rate variability and blood pressure during computer work. *European Journal of Applied Physiology*, vol. 92(1-2): pp. 84–89.

[17] HODGES, S., WILLIAMS, L., BERRY, E., IZADI, S., SRINIVASAN, J., BUTLER, A., SMYTH, G., KAPUR, N. and WOOD, K. (2006) SenseCam: a Retrospective Memory Aid. In *Proceedings of International Conference of Ubiquitous Computing*, 2006, pp. 177-193.

[18] INAN, O. T., ETEMADI, M., WIARD, R. M., GIOVANGRANDI, L., and KOVACS, G. T. (2009) Robust ballistocardiogram acquisition for home monitoring. *Physiological Measurement* vol. 30(2): pp. 169-185.

[19] KOTHARI, N., KANNAN, B., GLASGOW, E. D. and DIAS, M B. (2012) Robust Indoor Localization on a Commercial Smart Phone. *Procedia Computer Science* vol. 10: pp. 1114-1120.

[20] KWON, S., LEE, J., CHUNG, G. S. and PARK, K. S. (2011) Validation of heart rate extraction through an iPhone accelerometer. In *Proceedings of Engineering in Medicine and Biology Society*, pp. 5260-5263.

[21] LARA, O.D. and LABRADOR, M. A. (2013) A Survey on Human Activity Recognition using Wearable Sensors. In *IEEE Communications Surveys and Tutorials* vol. 15(3): pp.1192-1209.

[22] LUCAS, B. D. and KANADE, T. (1981) An Iterative Image Registration Technique with an Application to Stereo Vision. In *Proceedings of International Joint Conference on Artificial Intelligence*, pp. 674-679.

[23] MARCU, G., DEY, A. K. and KIESLER, S. (2012) Parent-driven Use of Wearable Cameras for Autism Support: a Field Study with Families. In *Proceedings of International Conference of Ubiquitous Computing*, pp. 401-410.

[24] MIGLIORINI M., BIANCHI A. M., NISTICÒ D., KORTELAINEN J., ARCE-SANTANA E., CERUTTI S., and MENDEZ M. O. (2010) Automatic sleep staging based on ballistocardiographic signals recorded through bed sensors. In *Proceedings of Engineering in Medicine and Biology Society*, pp. 3273-76.

[25] MOSES, Z. B., LUECKEN, L. J. and EASON, J. C. (2007) Measuring task- related changes in heart rate variability. In *Proceedings of Engineering in Medicine and Biology Society*, pp. 644-647.

[26] MORIGUCHI, A., OTSUKA, A., KOHARA, K., MIKAMI, H., KATAHIRA, K., TSUNETOSHI, T., HIGASHIMORI, K., OHISHI, M., YO, Y. and OGIHARA, T. (1992) Spectral change in heart rate variability in response to mental arithmetic before and after the beta-adrenoceptor blocker, carteolol. *Clinical Autonomic Research*, vol. 2(4): pp. 267–270.

[27] PAALASMAA J., WARIS M., TOIVONEN H., LEPPÄKORPI L., and PARTINEN M. (2012) Unobtrusive online monitoring of sleep at home. In *Proceedings of Engineering in Medicine and Biology Society*, pp. 3784-3788.

[28] PARAK, J. (2012) Heart Rate Detection from Ballistocardiogram. In *Proceedings of International Student Conference on Electrical Engineering*, vol. 1, pp. 1-5.

[29] PHAN, D. H., BONNET, S., GUILLEMAUD, R., CASTELLI, E. and THI, N. Y. P. (2008) Estimation of respiratory waveform and heart rate using an accelerometer. In *Proceedings of Engineering in Medicine and Biology Society,* pp. 4916-19.

[30] POH, M., MCDUFF, D. J. and PICARD, R. W. (2010) Non-contact, automated cardiac pulse measurements using video imaging and blind source separation. *Optics Express* vol. 18(10): pp. 10762–10774.

[31] POH, M., MCDUFF, D. J. and PICARD, R. W. (2011) Advancements in Noncontact, Multiparameter Physiological Measurements Using a Webcam. *IEEE Trans. on Biomedical Engineering,* vol. 58(1): pp. 7–11.

[32] PINHEIRO E., POSTOLACHE O., and GIRÃO P. (2010) Theory and developments in an unobtrusive cardiovascular system representation: ballistocardiography. *Open Biomedical Engineering*, vol. 4 (1), pp. 201-216.

[33] RIENZO, M. D., MERIGGI, P., VAINI, E., CASTIGLIONI, P. and RIZZO, F. (2012) 24h Seismocardiogram Monitoring in Ambulant Subjects. In *Proceedings of Engineering in Medicine and Biology Society,* pp.5050-5053.

[34] SHI, J. and TOMASI. C. (1994) Good features to track. *In Proceedings of IEEE Conference on Computer Vision and Pattern Recognition*, pp. 593-600.

[35] SHIN J. H., CHOI B. H., LIM Y.G., JEONG D. U., and PARK K. S. (2008) Automatic ballistocardiogram beat detection using a template matching approach. In *Proceedings of Engineering in Medicine and Biology Society*, pp. 1144-46.

[36] STARR, I., RAWSON, A. J., SCHROEDER, H. A. and JOSEPH, N. R. (1939) Studies on the estimation of cardiac output in man, and of abnormalities in cardiac function, from the hearts recoil and the bloods impacts: the ballistocardiogram. *The American Journal of Physiology*, vol. 127(1), pp. 1-28.

[37] TROSTER, G. (2005) The agenda of wearable healthcare. *IMIA Yearbook of Medical Informatics,* pp. 125-138.

[38] VERKRUYSSE, W., SVAASAND, L. O. and NELSON, J. S. (2008) Remote plethysmographic imaging using ambient light. *Optics Express* vol. 16(26): pp. 21434–21445.

[39] WU, H. Y., RUBINSTEIN, M., SHIH, E., GUTTAG, J., DURAND F., and FREEMAN, W. (2012) Eulerian Video Magnification for Revealing Subtle Changes in the World. *ACM Transactions on Graphics,* vol. 31 (4), pp. 1-8.